VERIZONA PUBLISHER
Publishing Your Ideas

www.verizonaonlinepublishing.com

Vol: 2, Issue: 1

Journal of Applied and Theoretical Physics Research

Proposal for an Easier Obtention of Piezoresistance Coefficients

Victor-Tapio Rangel-Kuoppa

Institut de Ciencia de Materials de Barcelona (ICMAB-CSIC), Campus UAB, Bellaterra, Spain

***Corresponding author:** Victor-Tapio Rangel-Kuoppa, Institut de Ciencia de Materials de Barcelona (ICMAB-CSIC), Campus UAB, Bellaterra, Spain; E mail: tapio.rangel@gmail.com

Article Type: Short Communication, **Submission Date**: 23 November 2017, **Accepted Date:** 22 December 2017, **Published Date:** 26 March 2018.

Citation: Victor-Tapio Rangel-Kuoppa (2018) Proposal for an Easier Obtention of Piezoresistance Coefficients. J Apl Theol 2(1): 17-21. doi: https://doi.org/10.24218/jatpr.2018.15.

Abstract

An alternative procedure to obtain the piezoresistance coefficients is proposed and implemented. It consists on the integration of the piezoresistance equation that relates the resistance change with the pressure change, *via* the piezoresistance coefficients. This yields a linear dependence between the logarithm of the measured resistance (R) and pressure (P). When implemented experimentally, this facilitates to make one single measurement of R vs P. The linear fit of the logarithm plot yields the piezoresistance coefficients. This technique is compared with the usual procedure, yielding smaller errors, while saving time and experimental and calculation effort, as only one measurement is necessary, as compared with the former procedure.

Keywords: Piezoresistance, Piezoresistance coefficients, Hydrostatic pressure.

The piezoresistance effect consists on the change of electrical resistance as function of pressure. In particular, in the semiconductor industry, it has important applications in Micro Electro Mechanical Systems (MEMS), such as sensors, accelerometers and solid-state joysticks [1].

These MEMS devices base their functionality on the fact, that in the case for semiconductors, the change of the resistivity tensor in a crystal can be written as a tensor equation related to the stress tensor as

$$\frac{\Delta \overleftrightarrow{\rho}}{\rho_0} = \overleftrightarrow{\pi}\,\overleftrightarrow{\sigma} \tag{1}$$

where $\Delta\overleftrightarrow{\rho}$, $\overleftrightarrow{\pi}$ and $\overleftrightarrow{\sigma}$ are the change of resistivity tensor, piezoresistance tensor and the stress tensor, respectively. Each one as dimensions of 3×3, 3×3×3×3 and 3×3, respectively while ρ_0 is the initial resistivity. Using crystal properties and symmetries, the notation can be collapsed and a simpler equation is obtained:

$$\frac{1}{\rho_0}\begin{pmatrix}\Delta\rho_1\\ \Delta\rho_2\\ \Delta\rho_3\\ \Delta\rho_4\\ \Delta\rho_5\\ \Delta\rho_6\end{pmatrix} = \begin{pmatrix}\pi_{11} & \pi_{12} & \pi_{12} & 0 & 0 & 0\\ \pi_{12} & \pi_{22} & \pi_{12} & 0 & 0 & 0\\ \pi_{12} & \pi_{12} & \pi_{22} & 0 & 0 & 0\\ 0 & 0 & 0 & \pi_{44} & 0 & 0\\ 0 & 0 & 0 & 0 & \pi_{44} & 0\\ 0 & 0 & 0 & 0 & 0 & \pi_{44}\end{pmatrix}\begin{pmatrix}\sigma_1\\ \sigma_2\\ \sigma_3\\ \sigma_4\\ \sigma_5\\ \sigma_6\end{pmatrix} \tag{2}$$

Further details about notation collapse and the use of the crystal symmetries can be found in Ref. 1, as they are not the intention of this article.

In particular, when stress is hydrostatic pressure, i.e., homogeneous and isotropic, then $\sigma_1 = \sigma_2 = \sigma_3 = -\Delta P$ and $\sigma_4 = \sigma_5 = \sigma_6 = 0$, and Eq. 3 becomes

$$\frac{1}{\rho_0}\begin{pmatrix}\Delta\rho_1\\ \Delta\rho_2\\ \Delta\rho_3\\ \Delta\rho_4\\ \Delta\rho_5\\ \Delta\rho_6\end{pmatrix} = \frac{1}{\rho_0}\begin{pmatrix}\Delta\rho\\ \Delta\rho\\ \Delta\rho\\ 0\\ 0\\ 0\end{pmatrix} = \begin{pmatrix}\pi_{11}+2\pi_{12}\\ \pi_{11}+2\pi_{12}\\ \pi_{11}+2\pi_{12}\\ 0\\ 0\\ 0\end{pmatrix}(-\Delta P) \tag{3}$$

Which becomes one single linear equation

$$\frac{\Delta\rho}{\rho} = \frac{\Delta R}{R} = -(\pi_{11}+2\pi_{12})\Delta P \tag{4}$$

where it has been used the fact that the resistivity is proportional to the measured resistance R. Also notice the minus sign that has been introduced in $\sigma_1 = \sigma_2 = \sigma_3 = -\Delta P$. This is due to the nature of hydrostatic pressure, which is a comprehensive stress, and thus, has a negative sign.

Hence, a piezoresistance measurement done with hydrostatic

pressure is a useful technique to obtain information about the piezoresistance coefficients π_{11} and π_{12}.

The standard procedure found in the literature is to measure the resistance R_0 at atmosphere pressure P_0, then increase pressure to different values of P_1, P_2, P_3, …. while measuring the respective R_1, R_2, R_3…. The respective $\Delta R_i = R_i - R_{i-1}$ and $\Delta P_i = P_i - P_{i-1}$ are obtained for each i = 1,2,3 measurement, and using Eq. 4, the value of $-(\pi_{11}+ 2\pi_{12})$ is obtained [1 -13].

This procedure has the inconvenience that the pressure should be set at certain value P_i, the resistance R_i measured at this value, and the respective $\Delta R_i = R_i - R_{i-1}$ and $\Delta P_i = P_i - P_{i-1}$ be calculated in order to use Eq. 4. A more convenient way to proceed would be a continuous change on the set pressure P while measuring continuously the resistance R. This second way to proceed would yield a more complete set of data, providing more information. It would be also very convenient if at the same time it could possible to avoid the calculation of ΔR_i and ΔP_i to obtain the piezoresistance coefficient, in order to save time and calculation efforts.

On what follows an alternative procedure to achieve this is proposed.

If the limit $\Delta P \to 0$ is done on Eq. 4, one obtains:

$$\frac{1}{R}\frac{dR}{dP} = \frac{d(lnR)}{dP} = -(\pi_{11} + 2\pi_{12}) \quad (5)$$

Integrating Eq. 5 respect to P, yields

$$lnR = -(\pi_{11} + 2\pi_{12})P + lnR_0 \quad (6)$$

Where R_0 is the resistance at atmosphere pressure.

Eq. 6 suggests that a continuous piezoresistance measurement can be done, increasing P from atmosphere pressure to larger values, while constantly measuring R. Once the measurement is done, the data are plot as $ln\ R$ vs P and the slope of the linear fit yields $-(\pi_{11}+ 2\pi_{12})$.

In order to implement this idea, a monocrystal of n-type <100>Si is used, as Si has been extensively studied [14,15]. Indium (In) was always used for ohmic contacts. Before any In soldering, the surface was slightly scratch with a knife to remove any native oxide. First, four soldered In ohmic contacts were done on the edge of a square sample, i.e, in van der Pauw geometry, such as Figure 1[16,17]. A Hall measurement was done and a resistivity of 110 mΩ×cm and an n-type charge carrier density of $n=8\times10^{16}$ cm^{-3} was obtained. This is in agreement with the reported electrical values of Si [18,19]. Afterwards a 2 mm × 4 mm slide was cut and four In soldered ohmic contacts where place on it, in the four probe configuration. Our sample was introduced in our Berilium high pressure cell, provided by the Institute of High Pressure Physics (IHPP, Warsaw, Poland). As recommended in their manual, a current of 10 μA was introduced on the edge In ohmic contacts, while measuring the voltage drop in the inner ohmic contacts, to measure the sample resistance. Pressure was varied from atmosphere pressure up to 1260 MPa. Measurements were done continuously, making time stops at pressures around 97, 122, 141, 157, 182, 204, 231, 258, 286, 318, 351, 388, 426, 467, 509, 557, 611, 661, 714, 770, 831, 890, 973, 1039, 1105, 1182 and 1260 MPa, as can be shown in Figure 1. This was done in order to obtain R_i resistance values at definite P_i pressures, to compare with the usual procedure that is done in the literature, as it is shown below.

In Figure 1 the measurement and its linear fitting are shown.

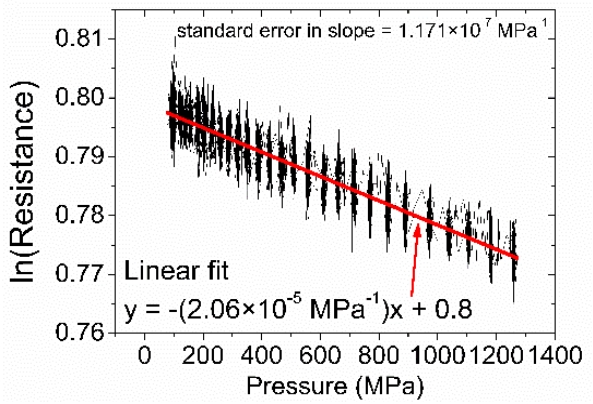

Figure 1: Resistance vs Pressure measurement. The linear fit is shown in red, yielding a slope of 2.06×10^{-5} $(MPa)^{-1}$

The linear fit yields a slope of 2.06×10^{-5} $(MPa)^{-1}$ with a standard error in slope of 1.171×10^{-7} $(MPa)^{-1}$.

The average R_i and P_i at each pressure stop were calculated, as their standard deviation, and they are shown in red in the following Figure 2. The linear fit to this average points is also shown.

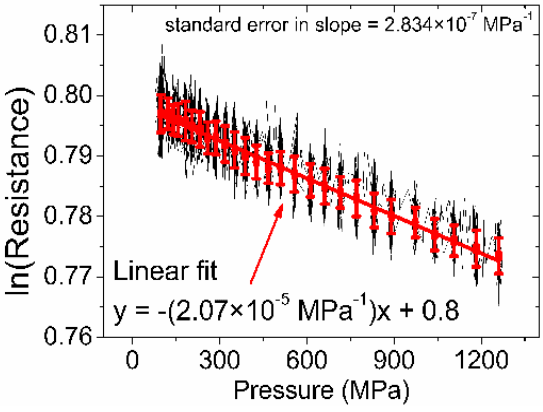

Figure 2: Average resistance vs average pressure measurement shown in red. The linear fit is shown in red as well, yielding a slope of 2.07×10^{-5} $(MPa)^{-1}$. The original measurement is shown in black

Finally, each value of and for each red point shown in Figure 2 are calculated, and they are shown in the Table 1. Also the value of is obtained and reported in Table 1, according to Eq. 4.

In Figure 3, the plot of Col. 6 (the piezoresistance term) vs Col. 2, is shown. Also, the linear fit is shown in red.

In Table 2, the results of the three procedures performed are summarized.

Citation: Victor-Tapio Rangel-Kuoppa (2018) Proposal for an Easier Obtention of Piezoresistance Coefficients. J Apl Theol 2(1): 17-21. doi: https://doi.org/10.24218/jatpr.2018.15.

Table 1: In Column (Col.) 1 the number of pressure stop is shown. Col. 2 and Col. 3 are the average pressure and resistance at each pressure stop. Col. 4 and Col. 5 are the calculated relative resistance change and pressure change between measurement at values *i* and *i-1*. Finally, Col. 6 is the piezoresistance term, calculated according to Eq. 4

Measurement ***i***	**Average Pressure** P_i **(MPa)**	**Average Resistance** R_i **(Ω)**	$\frac{\Delta R}{R_i} = \frac{Ri - R_{i-1}}{R_i}$	$\Delta P_i = P_i - P_{i-1}$ **(MPa)**	$-(\pi_{11}+2\pi_{12}) = \left(\frac{\Delta R}{R_i}\right)\left(\frac{1}{\Delta P_i}\right)$ **(×10^{-5}MPa^{-1})**
1	97.41	2.21882108			
2	122.02	2.21882108	0	24.61	0
3	141.08	2.21660343	-0.00099947	19.06	-5.2438
4	157.43	2.21660343	0	16.35	0
5	182.09	2.21613801	-0.00020997	24.66	-0.85147
6	204.13	2.21416658	-0.00088958	22.04738	-4.0348
7	231.62	2.21305981	-0.00049986	27.48262	-1.8188
8	258.92	2.20996378	-0.00139898	27.3	-5.1245
9	286.15	2.20996378	0	27.23	0
10	318.45	2.20775499	-0.00099947	32.3	-3.0943
11	351.77	2.20554841	-0.00099947	33.32	-2.9996
12	388.37	2.20334403	-0.00099947	36.6	-2.7308
13	426.01	2.20114185	-0.00099947	37.64	-2.6553
14	467.21	2.19894187	-0.00099947	41.2	-2.4259
15	509.33	2.19894187	0	42.12	0
16	557.32	2.1967441	-0.00099947	47.99	-2.0827
17	611.96	2.19454852	-0.00099947	54.64	-1.8292
18	661.15	2.19235513	-0.00099947	49.19	-2.0319
19	714.79	2.19016394	-0.00099947	53.64	-1.8633
20	770.07	2.18797494	-0.00099947	55.28	-1.808
21	831.37	2.18360349	-0.00199794	61.3	-3.2593
22	890.34	2.18142104	-0.00099947	58.97	-1.6949
23	973.16	2.17924078	-0.00099947	82.82	-1.2068
24	1039.65	2.17488678	-0.00199794	66.49	-3.0049
25	1105.98	2.17271305	-0.00099947	66.33	-1.5068
26	1182.59	2.16989044	-0.00129912	76.61	-1.6958
27	1260.27	2.16728821	-0.00119924	77.68	-1.5438

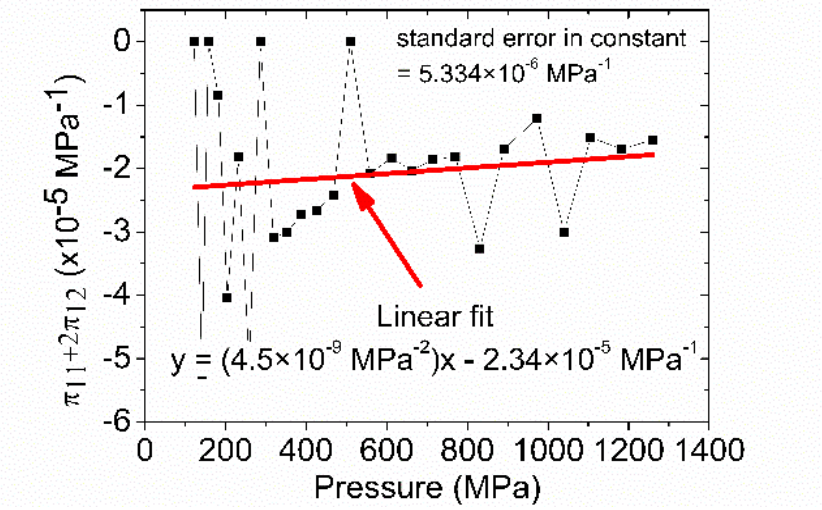

Figure 3: Plot of Col. 6 of Table 1 vs Col. 2 of Table 1. The linear fit is shown in red, yielding a constant term of 2.34×10^{-5} (MPa)$^{-1}$

Our results are compared with the results reported in the literature. In their study, Matsuda *et al.* reported the values of π_{11} and π_{12} for <100> n-type Si with charge carrier densities of $4x10^{16}$ cm^{-3}, 10^{17} cm^{-3} and $2x10^{18}$ cm^{-3}, and also the values reported by Smith *et al.* (see Table 3[14]). According to these values, the should have values of 2×10^{-5} MPa^{-1}, 1×10^{-5} MPa^{-1} and 1×10^{-5} MPa^{-1} for the n-type charge carrier densities of $4x10^{16}$ cm^{-3}, 10^{17} cm^{-3} and $2x10^{18}$ cm^{-3}. Using the values of Smith *et al.* [15], the value of should be 4×10^{-5} MPa^{-1}. The deduced values of this study (see Table 2) are in reasonable agreement with this reported value, especially for the case of $4x10^{16}$ cm^{-3}, which is very similar to the charge carrier density of our sample.

Finally, the experimental and analytical benefits of the proposed procedure of this study is commented. As it has been shown, a continuous measurement of resistance was done, as pressure was increased. All the measured data were used on the analysis, obtaining the piezoresistance coefficient $\pi_{11}+ 2\pi_{12}$ from the slope of the linear fit of the logarithm plot of the measured resistance vs pressure. For comparison, the same measurement was used in two different ways, to compare with the usual procedure found in the literature. In the first one, average resistance and average pressure points were calculated from the measurement, which was deliberately done stopping for some time at certain pressures. This average resistance and average pressures were used: a) as proposed in this article (see second row in Table 2) and b) as usually analysed in the literature (see third row in Table 2). This consumed experimental time and calculation effort, and, as can be seen from column 3 in Table 2, the standard error increased compared with this article's procedure proposal. It can also be seen in Figure 3 that the obtained piezoresistance coefficient $\pi_{11}+ 2\pi_{12}$ using the usual procedure done in the literature fluctuates in a wide range of values and several measurements are needed to obtain a reasonable average.

In summary, the procedure proposed here facilitates the obtention of piezoresistance coefficients, as a continuous resistance measurement can be done varying the pressure, and using a simple linear plot of all the measured data, the piezoresistance coefficients can be obtain with more accuracy than the procedure usually done.

Acknowledgements

The Consejo Superior de Investigaciones Cientificas (CSIC) from Spain and the Institut de Ciencia de Materials the Barcelona (ICMAB) are gratefully acknowledge for economical support

Table 2: Summary of results shown in Figure 1 to 3

Procedure	Piezoresistance term $(\pi_{11} + 2\pi_{12})$ (MPa^{-1})	Standard error (MPa^{-1})
This article procedure, using Eq. 6 on all measured data	2.06×10^{-5}	1.171×10^{-7}
This article procedure, using Eq. 6 on all averaged measurement points	2.07×10^{-5}	2.834×10^{-7}
Usual procedure done in the literature, using Eq. 4, [1-13]	2.34×10^{-5}	5.334×10^{-6}

References

1. Piezoresistivity in Microsystems. Jacob Richter, Technical University of Denmark; 2008.
2. Richter J, Arnoldus MB, Hansen O, Thomsen EV. Four point bending setup for characterization of semiconductor piezoresistance. Rev. Sci. Instrum. 2008; 79:044703.
3. Tufte ON, Chapman PW. Silicon diffused-element piezoresistive diaphragms. J. Appl. Phys. 1962; 33:3322.
4. Douglas MR. DMD reliability: a MEMS success story. Proceedings of SPIE – The International Society for Optical Engineering; 2003. 4980 p.
5. Alper SE, Azgin K, Akin T. A high-performance silicon-on-insulator MEMS gyroscopeoperating at atmospheric pressure. Sens and Act A Physical. 2007; 135(1):34-42. doi: https://doi.org/10.1016/j.sna.2006.06.043.
6. Abagal G. Electromechanical model of a resonating nano-cantilever-based sensor for highresolution and high-sensitivity mass detection. Nanotechnology. 2001; 12(2):100.
7. Edmiston J, Shkel Y. Piezoresistance in liquid suspensions: graphite in silicone elastomer. Phil. Mag. 2007; 87(17):2461-2481. doi: https://doi.org/10.1080/14786430701206666.
8. Bosseboeuf A, Allain PE, Parrian F, Le Roux X, Isac N, Jacob S, et al. Adv. Nat. Sci: Nanosci. Nanotechnol. 2015; 6:025001.
9. Arumugam S, Thiyagarajan R, Kalaiselvan G, Sivaprakash P. Pressure induced insulator-metal transition and giant negative piezoresistance in Pr 0.6 Ca 0.4 Mn 0.96 Al 0.04O3 polycrystal. J. Magn. Magn. Mater. 2016; 417:69-74. doi: http://dx.doi.org/10.1016/j.jmmm.2016.05.065.
10. Lee JH, Pin MW, Choi SJ, Jo MH, Shin J Ch, Hong SG, et al. Electromechanical Properties and Spontaneous Response of the Current in In As P Nanowires. Nano Lett. 2016; 16(11):6738-6745. doi: 10.1021/acs.nanolett.6b02155.
11. Wang J Ch, Karmakar RS, Lu YJ, Wu MCh, Wei K Ch. Nitrogen Plasma Surface Modification of Poly(3,4-ethylenedioxythiophene):Poly (styrenesulfonate) Films to Enhance the Piezoressitive Pressure-Sensing Properties. J. Phys. Chem. C. 2016; 120(45):25977-25984. doi: 10.1021/acs.jpcc.6b09642.
12. Gao D, YangZh, Zheng L, Zheng K. Piezoresistive effect of n-type <111>-oriented Si nanowieres under large tension/compression. Nanotechnology. 2017; 28(9):095702. doi: https://doi.org/10.1088/1361-6528/aa56ec.
13. Chauhan A, Taylor-Harrod I, Littlejohn SD, Nogaret A. Ultra Fast Pressure Sensing with Transient Tunnelling Currents. Nanoscale. 2017; 9(13):4544-4549. doi: 10.1039/c7nr01214d.
14. Matsuda K, Suzuki K, Yamamura K, Kanda Y. Nonlinear piezoresistance effects in silicon. J. Appl. Phys. 1993; 73(4):1838. doi: https://doi.org/10.1063/1.353169.

15. Smith Ch S. Piezoresistance Effect in Germanium and Silicoin. Phys. Rev. 1954; 94:42. doi: https://doi.org/10.1103/PhysRev.94.42.

16. Rangel-Kuoppa VT, Conde-Gallardo A. Ohmic contacts and n-type doping on TixCr2-xO3 films and the temperature dependence of their transport properties. Thin Solid Films. 2010; 519(1):453-456. doi: https://doi.org/10.1016/j.tsf.2010.07.087.

17. Rangel-Kuoppa VT, Conde-Gallardo A. Ohmic contact recipe on Ti x Cr 2− x O 3 and its application to temperature dependent Hall measurements. AIP Conf. Proc; 2013. 1566:23-24.

18. Rangel-Kuoppa VT, Chen G. Effects of several thermal glues used on temperature dependent Hall measurements. Rev. Sci. Instrum. 2010; 81(3):036102-036104. doi: 10.1063/1.3321563.

19. Rangel-Kuoppa VT, Chen G. Distortion Of Temperature Dependent Hall Measurements Due To Thermal Properties Of Thermal Glues. AIP Conf. Proc; 2011. 1399:1065-1066.